



Analysis of Milling Process of Aluminum Alloy Using Finite Element Method

Emil Nicusor Patru^(✉), Marin Bica, Nicolae Craciunoiu, Ionut Geonea,
Dumitru Panduru, and Leonard Ciurezu-Gherghe

Faculty of Mechanics, University of Craiova, 200512 Craiova, Romania
nick_emyl@yahoo.com

Abstract. Due to the tendencies to deform the component during milling process, and, as it is known, this can affect the dimensional characteristics, and not only, is very important to evaluate total deformation, equivalent elastic strain, equivalent stress, directional deformation, on X, Y and Z axis, shear elastic strain using the finite element analysis method for milling process of aluminum alloys.

In order to perform this analysis, a 3D model of the assembly is developed, with respect the real dimensions for each component, part and tool, respectively. Then, 3D model was transfer to the finite element analysis software, where, the results were obtained. For 3D model and finite element analysis, the dedicated software is used.

Keywords: Aluminum alloy · 3D model · Finite element analysis · Stress · Deformations

1 Introduction

Aluminum alloys are one of the most used materials in industry due to ability to combine the low weight with the good strength, and high strength-to-weight ratio can be an advantage to substitute steel and cast iron in the manufacture of many components. These properties make them widely used in automotive, shipping, aircraft industries, but also in the food industry and not only, [1, 2].

From point of view of machining, in a brief study [3, 4] the authors, study the machinability of the aluminum alloys, under aspects of tool wear, surfaces roughness, power consumption, tool conditions monitoring, cutting temperature, [3] or cutting forces, chip formation, dust emission, [4].

Finite element analysis is a well-known method to analyze different phenomena during cutting process as temperature, chip formation, stress, deformation etc.

In [5] the authors analyze, using finite element modeling, the influence of cutting speed, cutting edge inclination angle, tool rake and relief angles, and feed per tooth on cutting forces during high-speed milling of an aluminum alloy, while in [6] 3D finite element method is applied to simulate the influence of the tool helix angle in thin-wall milling process, also, of an aluminum alloy.

In [7] the authors used finite element method to broaden the possibilities of predicting the deflection of thin walls during milling of aluminum alloys.

In order to predict the distortion due to machining induced residual stress for a milled thin walled aluminum workpieces, 3D FEM cutting simulation is presented by the authors in [8].

In [9] finite element analysis is applied to study of burr formation in face milling of a cast aluminum alloy, and they use a tool with variable cutting edge radius and performance are compared with a conventional tool with uniform cutting edge radius.

Also, simulation, using the finite element method, with an adequate program, for analyze stress field and temperature field distribution, is presented by the authors in [10].

The main purpose of this analyze is to find the maximum values for stress and deformation during milling process of aluminum alloy using finite element method.

2 Analysis Details

2.1 Work-Piece Material and Milling Conditions

The materials used in this analysis, are, for work-piece, aluminum alloy, EN AW-6082 EN 485, with the mechanical properties, presented in Table 1 and chemical composition, in Table 2, and, for cutting tool, carbide alloy, with the mechanical properties, presented in Table 3.

Table 1. Mechanical properties of aluminum alloy, EN AW-6082

	Rm, MPa	Rp0,2 MPa	Elong. % 50 mm	HB
EN AW-6082	295	240	8	89

Table 2. Chemical composition of aluminum alloy, EN AW-6082

Si, %	Fe, %	C, %	Mn, %	Mg, %	Cr, %	Ni, %	Zn, %	Ti, %	Ga, %	V, %	Al
1.1	0.42	0.1	0.7	0.85	0.17	0.013	0.095	0.016	0.009	0.2	REM

Table 3. Mechanical and physical properties for carbide alloy

Ultimate strength, Rm, MPa	Young's modulus, E, GPa	Poisson's ratio	Density, Kg/m ³	Thermal expansion, 1/K	Specific Heat capacity, J/Kg-K
2600	800	0.22	14500	5.4·10 ⁻⁶	220

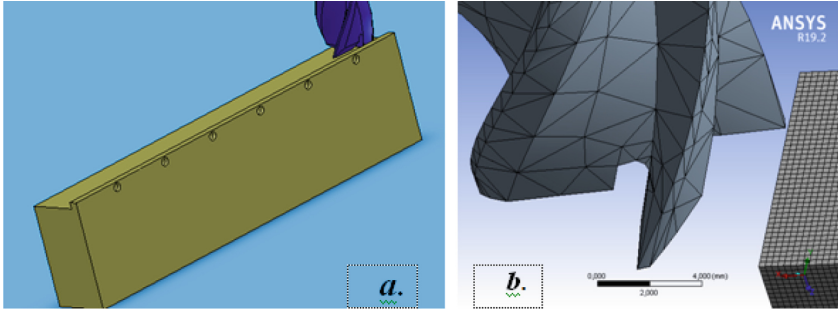


Fig. 1. 3D model for assembly workpiece-end mill; *a.* 3D model in SolidWorks; *b.* Assembly in Ansys Workbench, with the Mesh applied

3 3D Model of the Assembly Workpiece-Tool

In order to obtain the maximum values for stress and deformation during milling process of aluminum alloy, first, was necessary to develop the assembly workpiece-tool. For this purpose, a dedicated program for solid modeling, SolidWorks, Fig. 1, *a.*, was used, and then 3D model of the assembly was exported in Ansys Explicit Dynamics, where the Mesh was applied, Fig. 1, *b.*

Then, in order to perform the finite element analysis, Ansys Explicit Dynamics was used, following the well known steps: material properties both for tool and work-piece, defining the coordinated system, interaction between the bodies.

4 Results of Finite Element Analysis

After the steps presented bellow, next results were obtained. So, in Fig. 2, total deformation, *a.*, with the maximum value, 62.127, and equivalent elastic strain, *b.*, with the maximum value 0.87338 mm/mm, where is visible the chip formation (see detail, *c.*), are presented.

Figure 3 shows the equivalent stress, with the maximum value 180.65 MPa.

Directional deformation after X axis, is presented in Fig. 4, *a.*, after Y axis in Fig. 4, *b.*, and after Z axis in Fig. 4, *c.*, with the maximum values, respectively, 10.971, 10.973 and 2.9063, and as it is on the figure the minim value is after Z axis.

From point of view of maximum principal elastic strain, Fig. 5, *a.*, the maximum value is 0.70003 mm/mm, and minimum $3.4841 \cdot 10^{-5}$ mm/mm, Fig. 5, *b.*

For normal stress, Fig. 6, *a.*, and shear stress, Fig. 6, *b.* maximum obtained values are, 48.222 MPa, and 79.546 MPa, respectively.

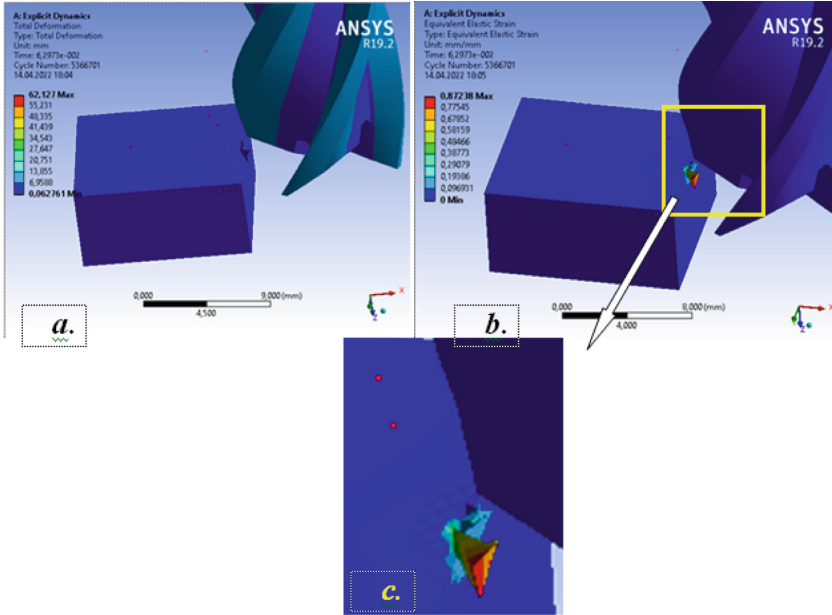


Fig. 2. Total deformation, *a*, and equivalent elastic strain, *b*, with the detail, *c*, to see the chip formation



Fig. 3. Equivalent stress, with the maximum value 180.65 MPa

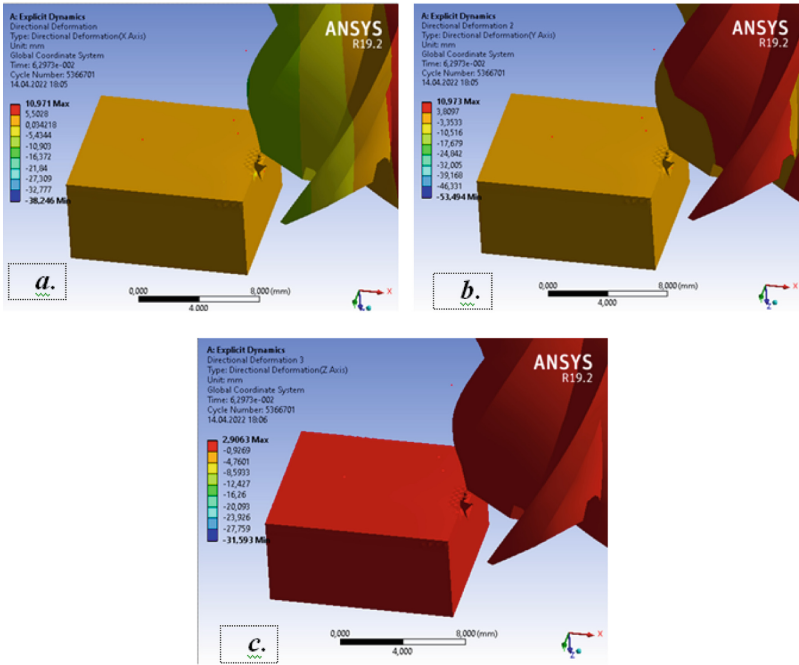


Fig. 4. Directional deformation, after X axis, *a.*, Y axis, *b.* and Z axis, *c.*

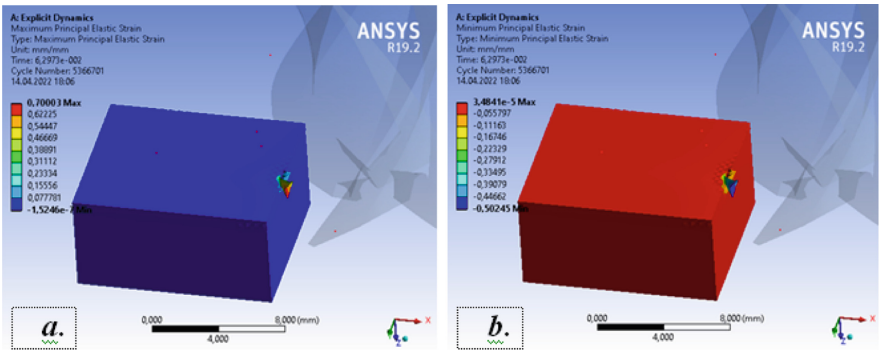


Fig. 5. Maximum, *a.*, and minimum values for principal elastic strain, *b.*

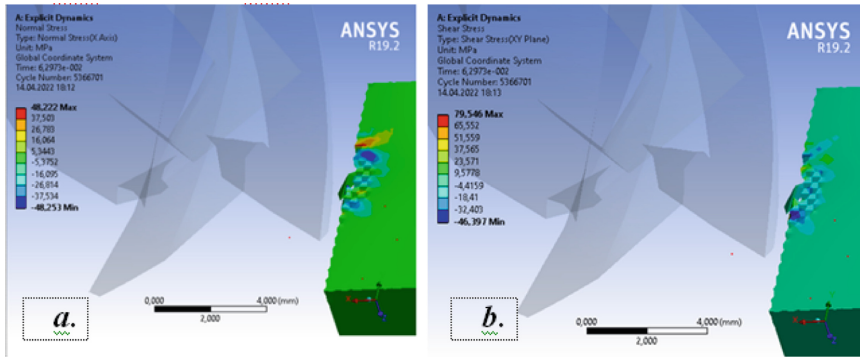


Fig. 6. Maximum values for normal stress, *a.* and shear stress, *b.*

5 Conclusions

In order to estimate total deformation, equivalent elastic strain, equivalent stress, directional deformation, on X, Y and Z axis, shear elastic strain using the finite element analysis method is applied for milling process of aluminum alloy. First, the model was developed in Solid Works, and then exported in Ansys Explicit Dynamics.

After define all the input data, material for cutting tool, for workpiece, with their mechanical properties, cutting parameters, meshing etc., the results of analysis was obtained and presented in Fig. 2 to Fig. 6. The values obtained, show the normal values, under the admissible values, for all data obtained.

From Fig. 2, the maximum values, for total deformation is 62.127, while the maximum value for equivalent elastic strain, is 0.87338 mm/mm, Fig. 3.

For directional deformation after X, Y and Z axis, Fig. 4, are, respectively, 10.971, 10.973 and 2.9063, with the maximum values in XOY plane, and minimum value after Z axis.

Maximum and minimum values for principal elastic strain, Fig. 5, are 0.70003 mm/mm, and $3.4841 \cdot 10^{-5}$ mm/mm, respectively.

Important are also, maximum values for normal stress, 48.222 MPa, and and shear stress, 79.546 MPa.

The present analysis was done just for one type of aluminum alloy, EN AW-6082 EN 485. In order to have more information about other types of aluminum alloys and to compare the results for the above results obtained for 6082 aluminum will be necessary, on the future, new finite element analysis applied to other aluminum alloy, like 5083, 7075 etc.

References

1. Jürgen HIRSCH, Recent development in aluminium for automotive applications, Trans. Nonferrous Met. Soc. China 24(2014) 1995–2002.
2. Burcu Ertuğ, Levent Cenk Kumruoğlu, 5083 type Al-Mg and 6082 type Al-Mg-Si alloys for ship building, American Journal of Engineering Research (AJER) e-ISSN : 2320–0847 p-ISSN : 2320–0936 Volume-4, Issue-3, 2015, pp-146–150.

3. Tusar Ranjan Soren, Ramanuj Kumar, Isham Panigrahi, Ashok Kumar Sahoo, Amlana Panda, Rabin Kumar Das, Machinability behavior of Aluminium Alloys: A Brief Study, *Materials Today: Proceedings* 18 (2019) 5069–5075.
4. V. Songmene, R. Khettabi, I. Zaghbani, J. Kouam, and A. Djebara, *Aluminium Alloys, Theory and Applications*, Chapter 18. *Machining and Machinability of Aluminum Alloys*, 2011, p. 377 – 400.
5. Xianghui Huang, Jinyang Xu, MingChen, FeiRen, Finite element modeling of high-speed milling of 7050-T7451 alloys, *Procedia Manufacturing* 43 (2020) 471–478.
6. G. Bolar, 3D Finite Element Method Simulations on the Influence of Tool Helix Angle in Thin-Wall Milling Process, *JJMIE*, Volume 16, Number 2, March. 2022 ISSN 1995-6665 Pages 283 – 289.
7. Czyzycki, J., Twardowski, P., Znojkwicz, N., Analysis of the Displacement of Thin-Walled Workpiece Using a High-Speed Camera during Peripheral Milling of Aluminum Alloys. *Materials* 2021, 14, 4771. <https://doi.org/10.3390/ma14164771>.
8. Daniel Weber, Benjamin Kirsch, Christopher R. Chighizola, Julianne E. Jonsson, Christopher R. D'Elia, Barbara S. Linke, Michael R. Hill, and Jan C. Aurich, Finite Element Simulation Combination to Predict the Distortion of Thin Walled Milled Aluminum Workpieces as a Result of Machining Induced Residual Stresses, 2nd International Conference of the DFG International Research Training Group 2057 – Physical Modeling for Virtual Manufacturing (iPMVM 2020), Article 11, p. 11:1–11:21.
9. Partchapol Sartkulvanich, Hakan Sahlan, Taylan Altan, A Finite Element Analysis of Burr Formation in Face Milling of a Cast Aluminum Alloy, *Machining Science and Technology*, 11:2, 157 – 181.
10. Yanzhong Zhang, Xiaohua Huang, Simulation and Research of Aerospace Material Milling Based On ABAQUS, 2020, *J. Phys.: Conf. Ser.* 1653 012070.

Open Access This chapter is licensed under the terms of the Creative Commons Attribution-NonCommercial 4.0 International License (<http://creativecommons.org/licenses/by-nc/4.0/>), which permits any noncommercial use, sharing, adaptation, distribution and reproduction in any medium or format, as long as you give appropriate credit to the original author(s) and the source, provide a link to the Creative Commons license and indicate if changes were made.

The images or other third party material in this chapter are included in the chapter's Creative Commons license, unless indicated otherwise in a credit line to the material. If material is not included in the chapter's Creative Commons license and your intended use is not permitted by statutory regulation or exceeds the permitted use, you will need to obtain permission directly from the copyright holder.

